Immunobiology 229 (2024) 152844

Contents lists available at ScienceDirect

Immunobiology

journal homepage: www.elsevier.com/locate/imbio

A study on the efficacy and Safety Evaluation of a novel PD-1/CTLA-4 bispecific antibody

Qi Song [a,b], Meiling Jiang [a], Xinrong Pan [a], Guanyue Zhou [a], Xiaomeng Zhang [a,*]

[a] Department of Pharmacology, SanHome, Nanjing, PR China
[b] College of Life Science and Technology, China Pharmaceutical University, Nanjing, PR China

ARTICLE INFO

Keywords:
Bispecific antibody
PD-1
CTLA-4
Immunotherapy
Safety

ABSTRACT

Tumors constitute a significant health concern for humans, and PD-1 and CTLA-4 monoclonal antibodies have been proven effective in cancer treatment. Some researchers have identified that the combination of PD-1 and CTLA-4 dual blockade demonstrates superior therapeutic efficacy. However, the development of PD-1/CTLA-4 bispecific antibodies faces challenges in terms of both safety and efficacy. The present study discloses a novel PD-1/CTLA-4 bispecific antibody, designated as SH010. Experimental validation through surface plasmon resonance (SPR) confirmed that SH010 exhibits favorable binding activity with both PD-1 and CTLA-4. Flow cytometry analysis demonstrated stable binding of SH010 antibody to CHOK1 cells overexpressing human or cynomolgus monkey PD-1 protein and to 293F cells overexpressing human or cynomolgus monkey CTLA-4 protein. Moreover, it exhibited excellent blocking capabilities in protein binding between human PD-1 and PD-L1, as well as human CTLA-4 and CD80/CD86. Simultaneously, in *vitro* experiments indicate that SH010 exerts a significant activating effect on hPBMCs. In murine transplant models of human prostate cancer (22RV1) and small cell lung cancer (NCI-H69), administration of varying concentrations of the bispecific antibody significantly inhibits tumor growth. MSD analysis revealed that stimulation of hPBMCs from three different donors with SH010 did not induce the production of cytokine release syndrome. Furthermore, Single or repeated intravenous administrations of SH010 in cynomolgus monkeys show favorable systemic exposure without noticeable drug accumulation or apparent toxicity. In conclusion, SH010 represents a novel cancer therapeutic drug poised to enter clinical trials and obtain market approval.

1. Introduction

The utilization of immune therapy approaches targeting the tumor immune escape mechanisms has emerged as a crucial component in clinical cancer treatment modalities(Shiroishi M, 2006). Currently, various inhibitors of immune checkpoints such as PD-1, PD-L1, and CTLA-4 have been approved for the treatment of multiple types of cancer (Mandel, et al., 2022, Valensa Yosephia, 2024). Monoclonal antibodies (mAbs) have emerged as a key and effective therapeutic modality in cancer treatment due to their ability to target specific molecules. However, monoclonal antibodies directed against a single target often fall short of achieving the necessary therapeutic effects due to the complex pathogenic mechanisms of cancer. Therefore, the development of antibodies targeting multiple targets has become a pivotal component of the next-generation therapeutic antibody landscape(Hosseini, et al., 2021).

PD-1 serves as a hallmark of tumor-infiltrating lymphocytes (TILs) with specificity for tumor-associated antigens(Gros, et al., 2014). The interaction between PD-L1-expressing tumor cells and immune cells expressing PD-1 generates signals through PD-1 binding to PD-L1/2, which can attenuate TCR signaling and negatively regulate T cell responses by dephosphorylating through the co-stimulatory receptor CD28(Freeman GJ, 2000, Hui E, 2017, Kamphorst, et al., 2017). Consequently, interrupting this signaling pathway can result in the restoration of T-cell functionality and the elicitation of an effective anti-tumor response.

The expression and function of CTLA-4 are closely associated with T-cell activation. CTLA-4 is rapidly upregulated following binding of the T-cell receptor (TCR), with its expression peaking 2–3 days after activation (Kennedy, et al., 2024, Pardoll, 2012). CTLA-4 competes with the co-stimulatory molecule CD28 for binding to the co-activating receptors CD80 and CD86 expressed on antigen-presenting cells. Through this

* Corresponding author.
E-mail address: zhangxm@sanhome.com (X. Zhang).

https://doi.org/10.1016/j.imbio.2024.152844
Received 8 February 2024; Received in revised form 22 July 2024; Accepted 23 August 2024
Available online 30 August 2024

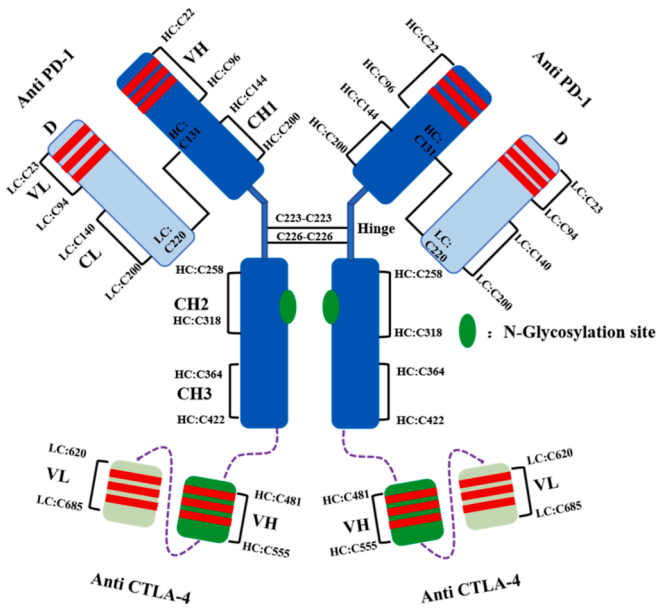

Fig.1. Schematic diagram of the SH010 structure.

competition, CTLA-4 modulates the activation and function of T cells by regulating the signaling intensity of the TCR/MHC complex(Qureshi, et al., 2011). CTLA-4 exhibits higher affinity in comparison to CD28 (Qureshi, et al., 2012). Therefore, CTLA-4, by modulating co-stimulatory signals provided by CD28, influences the initial activation of T cells and the activity of T cells in response to antigen presentation (Raskov, et al., 2020). This suggests that concurrently blocking PD-1 and CTLA-4 may yield a more potent anti-tumor effect. Multiple clinical trials have also confirmed this conclusion(Larkin, et al., 2015, Postow, et al., 2015, Wolchok, et al., 2013). Additionally, literature has already reported that PD-1 and CTLA-4 bispecific antibodies exhibit greater efficacy in *vitro* and in *vivo* compared to the combination of individual antibodies (Dovedi, et al., 2021, Pang, et al., 2023).

Currently, various bispecific anti-PD-1/CTLA-4 antibodies are also being described and tested in clinical trials(Dovedi, et al., 2021, Pang, et al., 2023, Perez-Santos, 2020). Recently, Cadonilimab has been approved for patients with recurrent or metastatic cervical cancer (Keam, 2022). Here, we present a novel targeted PD-1/CTLA-4 bispecific antibody, SH010. Through an in-depth investigation of the pharmacokinetics, immunological characteristics, and safety profile of SH010, we aim to provide a scientific basis for its prospective clinical application. We hope that this study will contribute to optimizing cancer immunotherapy strategies, enhancing treatment efficacy, and reducing potential risks.

2. Materials and methods

2.1. Cell lines

All cells were purchased from Chem Partner (CHOK1-hPD-1; CHOK1-cPD-1; 293F-hCTLA-4; 293F-cCTLA-4; 293F-blank). CHOK1-hPD-1 and CHOK1-cPD-1 are cultured in F12K (Gibco). 293F-h/cCTLA-4 is cultured in DMEM (Corning). CHOK1-blank was purchased from ATCC. hPBMCs were purchased from WuXi AppTec (Donor 1:20062778, Donor 2:20061463, Donor 3:20061483, Donor 4:20200017, Donor 5:20200020, Donor 6:20200041). Human prostate cancer cells 22RV1 and human small cell lung cancer cells NCI-H69 were purchased from ATCC. All cells were cultured at 37 ∘C in a humidified chamber with 5 % CO_2.

2.2. Surface plasmon resonance (SPR)

SPR experiments were performed on a Biacore 8 K instrument using a CM5 (GE Healthcare) at 25 °C. Filtered HBS-EP (GE Healthcare) was used as the running buffer. HBS-EP buffer containing 500 mM NaCl (Sigma) and 2 % (w/v) bovine serum albumin (BSA, Gibco) was used as the dilution solution. The diluted SH010 candidates were captured on the surface of CM5 chip. The histidine-tagged human PD-1 (Sino Biological) and Cynomolgus Monkey PD-1 (Sino Biological) were diluted serially with a running buffer from 100 nM to 3.125 nM. The histidine-tagged human CTLA-4 (Sino Biological) and Cynomolgus Monkey CTLA-4 (Sino Biological) were serially diluted with the running buffer from 100 nM to 3.125 nM. Data analysis was performed using Biacore Insight Evaluation Software (GE Healthcare).

2.3. Targeted binding and blocking were studied by flow cytometry

The binding of the SH010 antibody to CHOK1-PD-1 (human or cynomolgus monkey) and 293F-CTLA-4 (human or cynomolgus monkey) cell lines was analyzed by cytometry (BD Biosciences). Cells were collected and diluted antibody (starting from 10 μg/mL) was added to each well. After thorough mixing, the mixture was incubated at 4 °C for 1 h. Working solution containing Alexa 488-labeled goat anti-human IgG (H+L) (Life Technology) and FACS buffer (diluted 1:1000) was added to each well. After incubation, cells were washed and resuspended in FACS buffer, then data were acquired using a flow cytometer. The EC_{50} values are calculated using GraphPad Prism software.

All recombinant proteins were purchased from Sino Biological (human PD-L1: 10084-H08H, human B7-1: 10698-H08H, human CD86: 100699-H08H). To block the binding of human PD-L1 protein to CHOK1-hPD-1 cells, diluted antibody was mixed with 93.75 μg/mL hPD-L1 protein (final concentration: SH010 antibody and hIgG4 50 μg/mL). To block the binding of human B7-1 and human CD86 proteins to 293F-hCTLA-4 cells, diluted antibody was mixed with 7.64 μg/mL hB7-1 and 30.88 μg/mL hCD86 protein, respectively (final concentration: SH010 antibody 250 μg/mL, hIgG4 antibody 187.5 μg/mL; hB7-1 and hCD86 protein concentrations were 3.82 μg/mL and 15.44 μg/mL, respectively). Each well was incubated with His-tag antibody (GenScript) diluted in FACS buffer (1:500) at 4 °C in the dark for 30 min. After incubation, cells were washed and resuspended in FACS buffer, then data were acquired using a flow cytometer. The IC_{50} values are calculated using GraphPad Prism software.

2.4. ELISA detected the effect of hPBMCs on SEB stimulation

Resuscitate hPBMCs and count using a Cell Counter (Beckman). hPBMCs (HemaCare) were thawed and counted using a cell counter (Beckman). The counted hPBMCs were seeded into 96-well U-bottom plates (Corning), followed by addition of SH010, Nivolumab (BMS), and hIgG4 (Sino Biological). After incubation, Staphylococcal enterotoxin B (SEB) was added (final concentration 100 ng/ml). The 96-well plates (Axygen) were coated with 0.5 μg/mL of protein overnight at 4 °C. Blocking buffer containing 1 % BSA (Gibco) was added to block nonspecific binding. Subsequently, antibodies were added and incubated, followed by addition of horseradish peroxidase (HRP)-conjugated goat anti-human IgG Fc or F(ab')2 secondary antibodies (Pierce) for incubation at 37 °C. Finally, HRP substrate 3,3′,5,5′-tetramethylbenzidine (TMB; Sigma) was added for color development. Absorbance at 450 nm was measured using a microplate reader (Molecular Devices). Statistical analysis was performed using GraphPad Prism software.

2.5. In vivo mouse study to evaluate therapeutic efficacy

Female huPBMC-NCG mice generated by Biocytogen (Jiangsu, China) were subcutaneously injected with human small-cell lung cancer cells NCI-H69 (5×10^6 cells). When the tumor size reached ~ 120 mm^3,

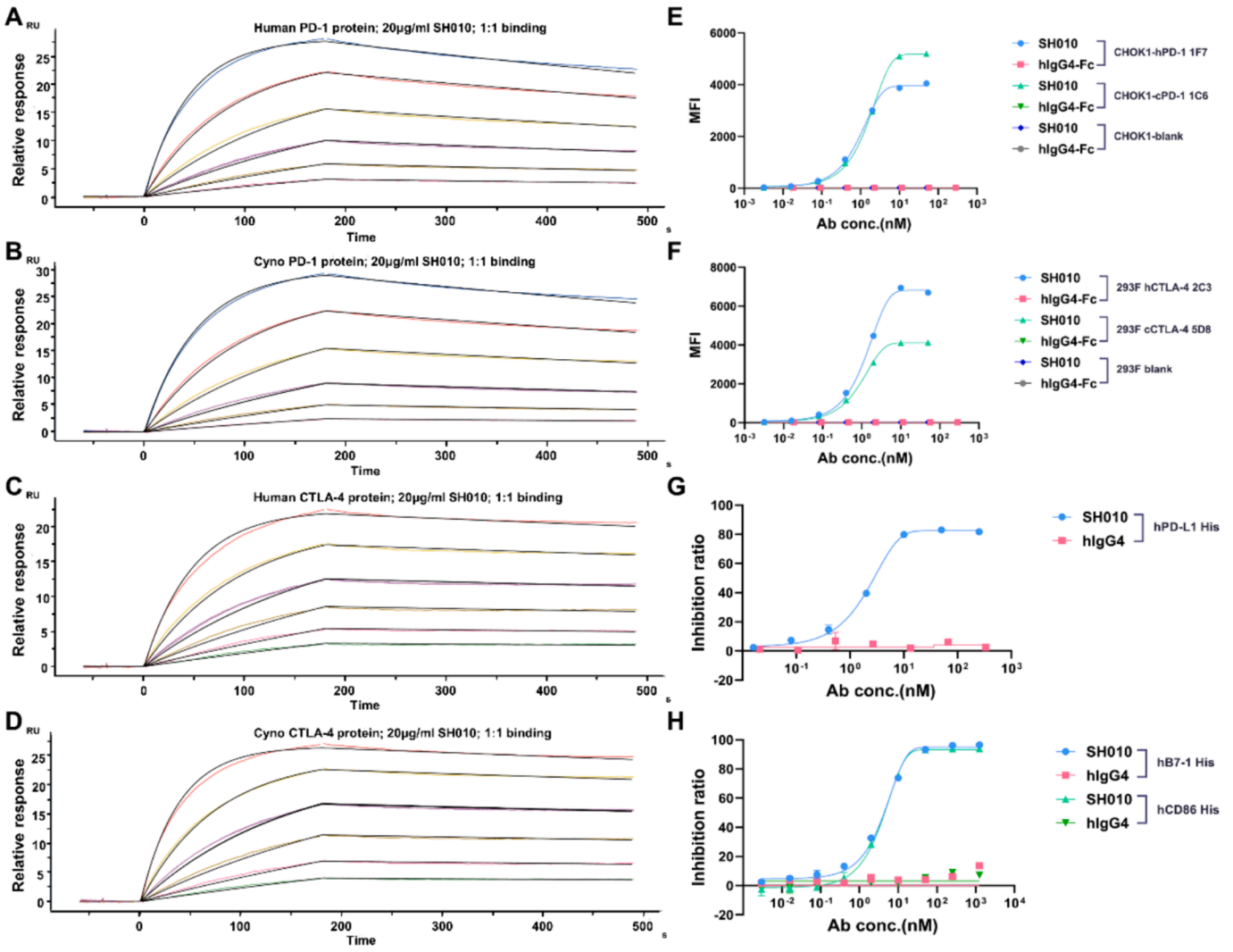

Fig.2. Study of SH010 Antibody Characteristics. Binding of SH010 with Human PD-1 (A), Cynomolgus Monkey PD-1 (B), Human CTLA-4 (C), and Cynomolgus Monkey CTLA-4 (D); Binding of SH010 with CHOK1-h/cPD-1 (E) and 293F-h/cCTLA-4 (F) Cell Lines; SH010 Antibody Blocking of Human PD-1 and PD-L1 Interaction (G); SH010 Antibody Blocking of Human CTLA-4 and B7-1/CD86 Interaction (H). Nonlinear regression analysis was also performed using a sigmoidal four-parameter logistic model in GraphPad Prism.

tumor-bearing animals were randomly enrolled into different study groups. Groups of 8 animals were intravenously administered 20 mg/kg Nivolumab or 13.3 or 26.6 mg/kg SH010, twice a week. Tumor volume and survival were monitored and recorded twice per week. The experiment was terminated after three weeks of drug treatment.

Male huPBMC-NCG mice generated by Biocytogen (Jiangsu, China) were subcutaneously injected with human prostate cancer cells 22RV1 (5×10^6 cells). When the tumor size reached ~ 120 mm^3, tumor-bearing animals were randomly enrolled into different study groups. Groups of 10 animals were intravenously administered 10 mg/kg Nivolumab or 13.3 mg/kg SH010, twice a week. Tumor volume and survival were monitored and recorded twice per week. The experiment was terminated after three weeks of drug treatment. Statistical analysis was performed using GraphPad Prism software.

2.6. Study on pharmacokinetics of cynomolgus monkey

Single intravenous infusion of SH010 was administered in groups comprising 3 male and 3 female cynomolgus monkeys. The experimental animals in each group underwent a slow intravenous injection of SH010 at doses of 10, 30, or 90 mg/kg, and blood samples were collected from the peripheral veins at nine-time points (hours 0.5, 1, 2, 8, 24, 72, 120, 216, and 312) post-administration. The collected blood samples were analyzed using the enzyme-linked immunosorbent assay (ELISA) method. For repeated intravenous infusions of SH010, each group included 5 male and 5 female cynomolgus monkeys. The animals in each group received a slow intravenous injection of SH010 at doses of 10, 30, or 100 mg/kg, once a week, on the 1st and 22nd days, and blood samples were collected from the peripheral veins at seven-time points (hours 0.5, 2, 8, 24, 72, 120, and 168) post-administration. The collected blood samples were analyzed using the ELISA method. This monkey study adhered to the Safety and Quality Assurance guidelines outlined in the Guideline for Experiments Document of WuXi AppTec.

2.7. Safety assessment of SH010

Each experimental group comprised five male and five female cynomolgus monkeys. The groups received a slow intravenous injection of SH010 at doses of 10, 30, or 100 mg/kg once weekly for four administrations on days 1, 8, 15, and 22. Body weight was measured at nine time points (days 0, 7, 14, 21, 28, 35, 42, 49, and 57). Concurrently, blood samples (1.0 mL each) were collected via the cephalic or femoral vein, and within 2 h, lymphocyte percentages, including total T cells, CD8 + T cells, CD4 + T cells, NK cells, and B cells, were assessed using flow

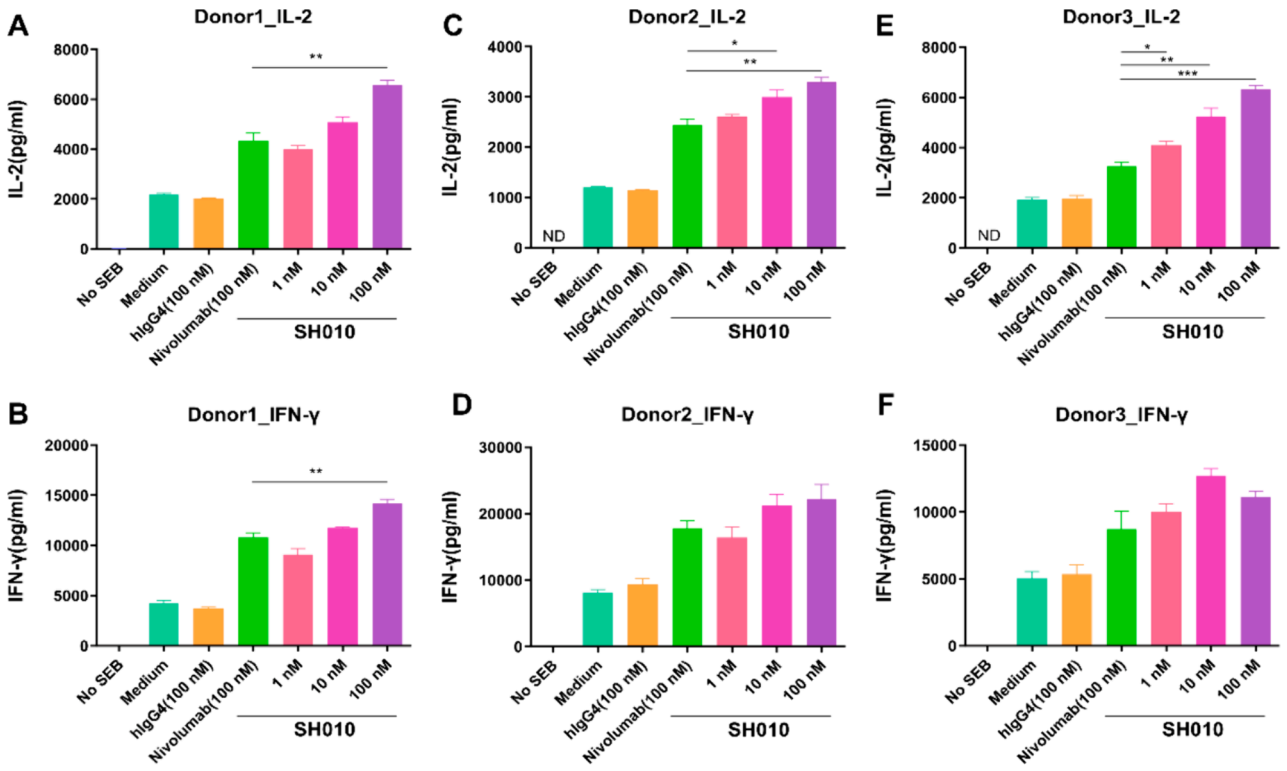

Fig.3. SH010 enhances the activity of hPBMCs stimulated by SEB. The impact of SH010 on IL-2 secretion by SEB-stimulated hPBMCs in donors 1 (A), 2 (C), and 3 (E). The influence of SH010 on IFN-γ secretion by SEB-stimulated hPBMCs in donors 1 (B), 2 (D), and 3 (F). Nivolumab serves as a positive control, and hIgG4 serves as an isotype control. One-way analysis of variance followed by Dunnett's multiple comparisons test compared with control hIgG4. *P<0.05.

cytometry. This monkey study adhered to the Safety and Quality Assurance guidelines outlined in the Guideline for Experiments Document of WuXi AppTec.

Antibody coating solution (Sigma-Aldrich) was prepared by diluting SH010 and IgG4 to concentrations of 0.1 μg/mL, 1 μg/mL, 10 μg/mL, and 100 μg/mL. SH010 and IgG4 were separately added to 96-well plates and then incubated overnight at 4 °C. Afterward, the plates were washed with PBS (Thermo). Human peripheral blood mononuclear cells (hPBMCs) were evaluated for cell viability and counted, then diluted to an appropriate concentration. The hPBMCs cell suspension was added to a 96-well round-bottom culture plate (liquid phase method) and a 96-well flat-bottom culture plate containing the test antibodies (solid-phase method). The cells were cultured at 37 °C with 5 % CO_2 for 4 h, 24 h, and 48 h. The cell-free supernatants were used for subsequent Meso Scale Discovery (MSD) assays. The results were analyzed using MSD Discovery Workbench and GraphPad Prism software.

2.8. Statistical analyses

Results are presented as mean ± SEM. Statistical analyses were carried out using GraphPad Prism software (GraphPad Software, San Diego, CA, USA). Statistical significance for tumor volume between groups was determined by one-way ANOVA, and $p < 0.05$ were considered to be statistically significant. Asterisks indicate statistical compared to PBS group unless otherwise indicated in the figures (*$p < 0.05$, **$p < 0.01$,). Tumor volume was calculated as (small diameter^2 × large diameter)/2. Tumor growth inhibition (TGI) was calculated by the following formula: 100-(group average tumor weight/control average tumor weight) × 100. Using WinNonlin Version 6.3 or later (Pharsight) pharmacokinetic software, process the serum concentration data of SH010 with a non-compartmental model. Calculate the relevant pharmacokinetic parameters using the linear log trapezoidal method. The phenotyping of immune cells was analyzed using one-way ANOVA, comparing the results to Day 0. Cytokine release was analyzed using one-way ANOVA, with comparisons made to the control hIgG4.

3. Result

3.1. Characterization of SH010 antibody

SH010 is a bispecific antibody targeting human CTLA-4/PD-1 produced through recombinant DNA technology in Chinese hamster ovary (CHO) cells. This antibody comprises two symmetrical chains forming a homodimer, totaling 1848 amino acids, with the heavy chain consisting of 704 amino acids and the light chain consisting of 220 amino acids. Fusion of scFv at the Fc end is achieved through a linker (GGGGS)3, connecting the heavy chain variable region and the light chain variable region with a linker (GGGGS)4. Moreover, the variable region of the antibody is humanized. SH010 possesses a total of 16 intrachain disulfide bonds and 4 interchain disulfide bonds. The N-glycosylation site is located on the heavy chain at the 294th asparagine residue (indicated by the green region in Fig. 1).

The binding affinity of SH010 was evaluated using surface plasmon resonance (SPR) to assess its interaction with various antigens, specifically PD-1/CTLA-4. The results showed that SH010 had similar binding strength with human and cynomolgus monkey PD-1 proteins, with KD values of 3.33 nM (Fig. 2A) and 3.31 nM (Fig. 2B), respectively. Similarly, SH010 demonstrated equivalent binding affinity with human and cynomolgus monkey CTLA-4 proteins, with KD values of 0.688 nM (Fig. 2C) and 0.484 nM (Fig. 2D), respectively. However, SH010 did not show any binding to mouse and rat PD-1 and CTLA-4 proteins (Supplementary Fig.S1). The binding affinity of SH010 to PD-1 or CTLA-4 from various species was assessed using flow cytometry. The results demonstrated that SH010 exhibited similar binding affinities to stably overexpressed human and cynomolgus monkey PD-1 proteins in CHOK1 cells, with EC50 values of 0.895 nM and 1.627 nM, respectively (Fig. 2E). Additionally, SH010 displayed comparable binding affinities

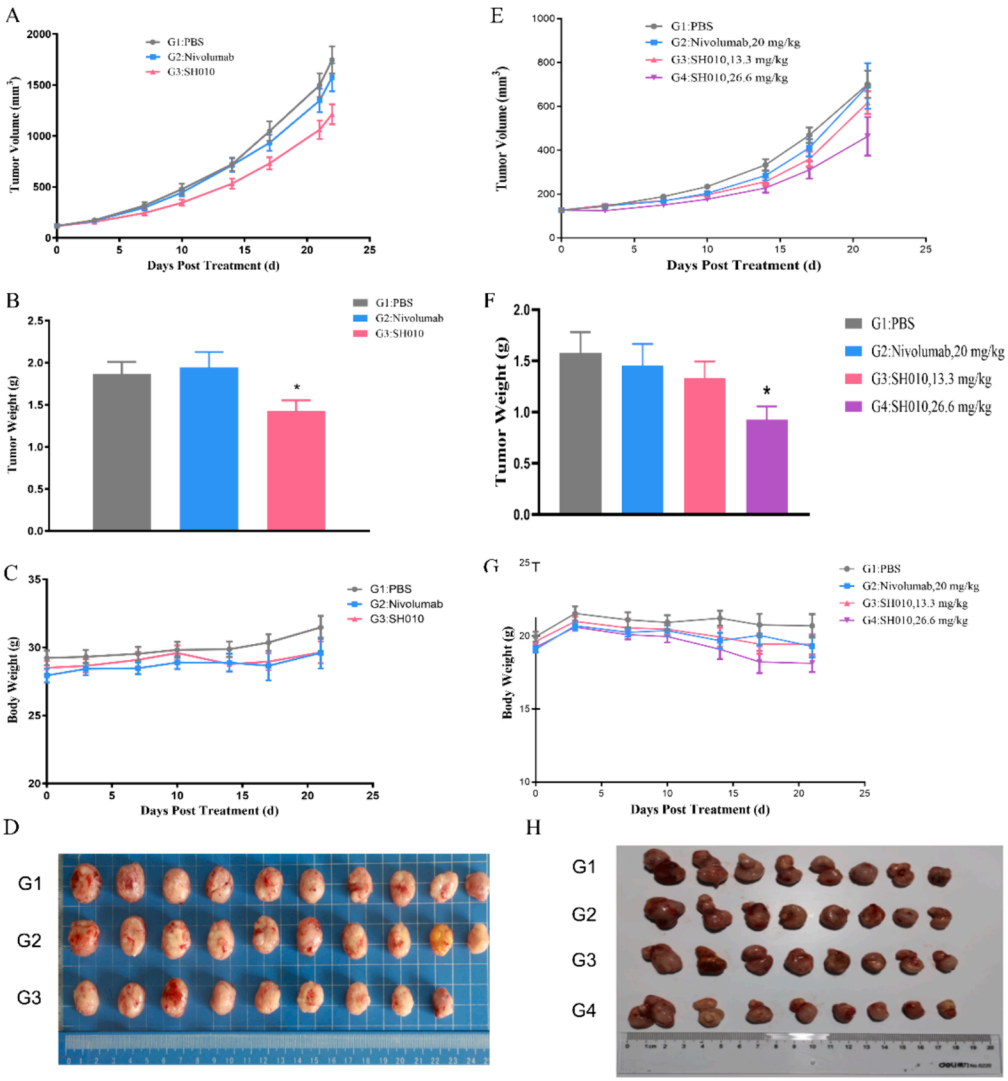

Fig.4. Inhibitory Effect of SH010 in tumor xenograft models. The impact of SH010 on the growth of transplanted tumors derived from 22RV1 in mice, assessing tumor volume (A) and tumor weight (B) (n = 10). Changes in body weight of mice with transplanted tumors derived from 22RV1 (C) and NCI-H69 (G) treated with SH010. The influence of SH010 on the growth of transplanted tumors derived from NCI-H69 in mice, evaluating tumor volume (E) and tumor weight (F) (n = 8). Photographs of mouse tumor models 22RV1 (D) and NCI-H69 (H). All data are presented as the mean ± standard error of the mean (SEM) or mean ± standard deviation (SD).

to stably overexpressed human and cynomolgus monkey CTLA-4 proteins in 293F cells, with EC50 values of 1.222 nM and 0.898 nM, respectively (Fig. 2F). The inhibitory effects of the SH010 antibody on the interactions between human PD-1 and PD-L1, as well as human CTLA-4 and CD80/CD86, were evaluated using flow cytometry. The results indicated that SH010 effectively inhibited the binding of stably overexpressed human PD-1 protein in CHOK1 cells to human PD-L1 his protein, with an IC50 value of 2.246 nM (Fig. 2G). Moreover, SH010 blocked the binding of stably overexpressed human CTLA-4 protein in 293F cells to human CD80 his protein and human CD86 his protein, with IC50 values of 3.980 nM and 3.549 nM, respectively (Fig. 2H).

3.2. SH010 enhances the activity of hPBMCs stimulated by SEB

The secretion of IFN-γ/IL-2 is an important indicator of lymphocyte activation. To assess the impact of varying concentrations of SH010 on the secretion of interferon-γ (IFN-γ) and interleukin-2 (IL-2) from hPBMCs stimulated with SEB, ELISA was employed for detection. Treating hPBMCs with SEB at 100 ng/mL for 72 h significantly increased the secretion of IFN-γ/IL-2. Across three donors, SH010 demonstrated a concentration-dependent promotion of cytokine secretion. Moreover, there was a significant difference in the IL-2 release levels between the SH010 treatment group and the Nivolumab group across the three donors (Fig. 3A, 3C, 3E, $P<0.05$).

3.3. Inhibition of tumor growth in huPBMC-NCG mice by SH010

Utilizing the 22RV1 prostate cancer cell xenograft model, when the mean initial tumor volume reached 117.60 mm^3, hPBMCs were administered. Subsequently, solvent, Nivolumab, and SH010 were intravenously injected twice a week. The inhibitory effect of SH010 on tumor growth in huPBMC-NCG mice was observed. The results indicated that, compared to the control group, the tumor volume inhibition rate (TGI_{TV}) for the Nivolumab group (G2, 10 mg/kg) was 10.49 % (Fig. 4A, $P>0.05$), and the tumor weight inhibition rate (TGI_{TW}) was −4.03 % (Fig. 4C, $P>0.05$). However, the SH010 group (G3, 13.3 mg/kg) exhibited a significant tumor volume inhibition rate of TGI_{TV}=32.66 % (Fig. 4A, $P<0.01$) and a tumor weight inhibition rate of TGI_{TW}=23.85 % (Fig. 4B, $P<0.05$). Additionally, there was a slight increase in mouse body weight, with no significant differences observed among the groups

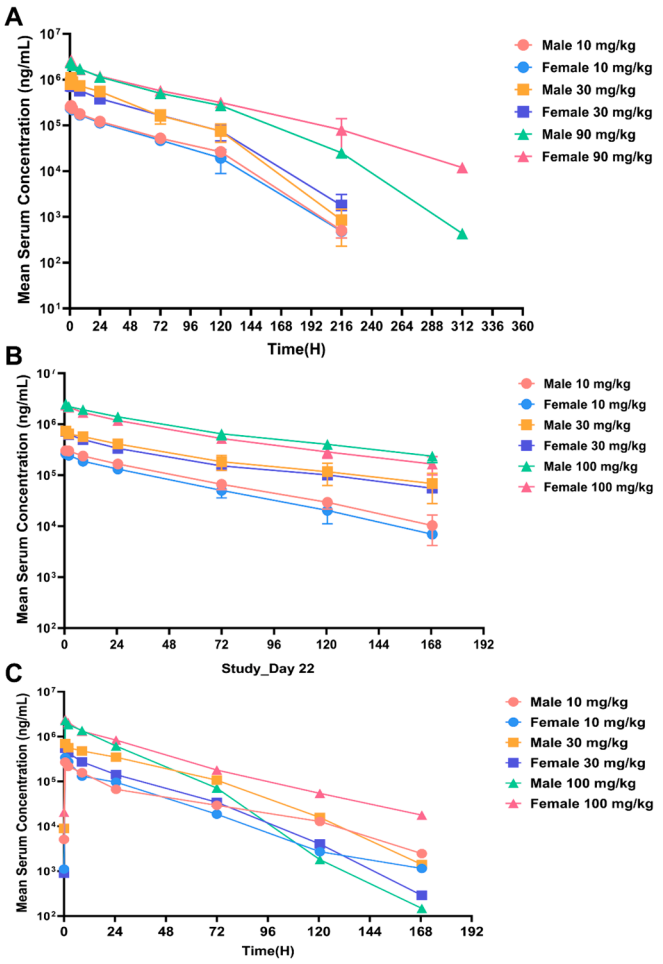

Fig.5. Pharmacokinetic Study of Intravenous Infusion of SH010 in cynomolgus Monkeys. (A) Mean serum concentration–time curves of SH010 following a single intravenous infusion in male and female cynomolgus monkeys (n = 3). (B) Average concentration–time profiles of SH010 on Day 1 and (C) Day 22 after repeated intravenous infusions of SH010 in male and female cynomolgus monkeys (n = 5).

(Fig. 4C, P>0.05).

In the NCI-H69 small cell lung cancer cell xenograft model, when the mean initial tumor volume reached 120 mm^3, hPBMCs were administered, and solvent, Nivolumab, and SH010 were intravenously injected twice a week. The inhibitory effect of SH010 on tumor growth in huPBMC-NCG mice was observed. The results indicate that on the 21st day of administration, there was a significant reduction in tumor volume across all treatment groups, with the G4 group (SH010, 26.6 mg/kg) exhibiting the most notable effect, showing a relative tumor volume inhibition rate of 41.40 % (Fig. 4D, P<0.05). Furthermore, there was a strong correlation between tumor volume and drug concentration. In the final tumor weight analysis for each group, compared to G1 (Control group), G2 (Nivolumab, 20 mg/kg), and G3 (SH010, 13.3 mg/kg) showed no significant differences in tumor weight. However, G4 (SH010, 26.6 mg/kg) exhibited a significant difference compared to G1 (Control group) (Fig. 4E, P<0.05). There was no significant decrease in animal body weight, indicating good tolerance in the mice (Fig. 4F).

These findings indicate that SH010 at 13.3 mg/kg effectively inhibits the growth of subcutaneously transplanted 22RV1 human prostate cancer cells in huPBMC-NCG mice, while Nivolumab at 10 mg/kg did not show significant tumor inhibition. Simultaneously, SH010 at 26.6 mg/kg demonstrated a pronounced antitumor effect in the NCI-H69 small cell lung cancer cell xenograft model in huPBMC-NCG mice. SH010 exhibited its therapeutic effect without inducing toxic side effects, demonstrating good safety.

3.4. Pharmacokinetic study of intravenous infusion of SH010 in cynomolgus monkeys

After a single intravenous infusion of SH010 at doses of 10, 30, and 90 mg/kg in male and female cynomolgus monkeys, there were no apparent gender differences in systemic exposure ($AUC_{0\text{-last}}$ and C_{max}) at each intravenous dose. As the intravenous dose increased from 10 to 30 mg/kg, 30 to 90 mg/kg, and 10 to 90 mg/kg, the systemic exposure of SH010 in both male and female cynomolgus monkeys increased proportionally to the dose (Fig. 5A). Upon repeated intravenous administration of SH010 at doses of 10, 30, or 100 mg/kg in male and female monkeys, based on the change in $AUC_{0\text{-}168.5h}$, there was no significant drug accumulation observed in male monkeys at the 30 mg/kg and in female monkeys at the 100 mg/kg. However, a decrease in systemic exposure was noted in male and female monkeys at the 10 mg/kg, in female monkeys at the 30 mg/kg, and in male monkeys at the 100 mg/kg (Fig. 5B, 5C).

3.5. Safety assessment of SH010

The average body weight of female (Fig. 6A) and male (Fig. 6B) cynomolgus monkeys, subjected to repeated intravenous administration of SH010 for 29 days followed by a 28-day recovery period, exhibited no significant alterations. Additionally, there were no discernible differences in body weight between females and males. Moreover, there were no discernible differences between males and females. On the 30th day, compared to the control group and pre-treatment levels, there were no apparent changes in the percentages of CD4 + T ($CD45^+CD3^+CD4^+CD8^-$) cells (Fig. 6E) and B ($CD45^+CD3^-CD16^-CD20^+$) cells (Fig. 6G) among lymphocytes. However, a significant reduction in the percentage of NK ($CD45^+CD3^-CD16^+CD20^-$) cells (Fig. 6F) among lymphocytes was observed in the treated groups, particularly in the high-dose group. Notably, a pronounced decrease in the percentages of total T ($CD45^+CD3^+$) cells (Fig. 6C) and CD8+ ($CD45^+CD3^+CD4^-CD8^+$) T cells (Fig. 6D) among lymphocytes was observed in the high-dose male group. These cellular changes returned to pre-treatment levels on Day 57. The impact of SH010 on the secretion of cytokines (IFN-γ, TNF-α, IL-2, IL-4, IL-6, IL-8, IL-10) by hPBMCs post-stimulation was assessed using MSD. In the solid-phase detection system, SH010 induced TNF-α release in hPBMCs from all three donors (Fig. 6H, 6I, 6 J). In the liquid-phase detection system, SH010 triggered IL-6 release in Donor 5 at 24 h and 48 h (Fig. 6L) and IL-10 release at 48 h (Fig. 6K). Furthermore, SH010, at various concentrations and treatment durations, elicited levels of other cytokines secreted by hPBMCs comparable to those in the IgG4 group under equivalent stimulation conditions (Supplementary Fig.S3, S4, S5).

4. Discussion

James P. Allison and Tasuku Honjo were awarded the 2018 Nobel Prize in Physiology or Medicine for their discovery of a method for treating cancer by inhibiting negative immune regulation. Their research on the immune checkpoint PD-1 and CTLA-4 showed that they act as “brakes” in immune function and indicated that immune checkpoint inhibition may reactivate T cells to more effectively eliminate cancer cells(Ljunggren, et al., 2018). Studies have shown that the blockade of CTLA-4 primarily regulates the activation of T cells in lymph nodes and suppresses DC activity through Treg cells and that it will work synergistically with the blockade of PD-1, which primarily involves the inhibition of activation of effector T cells and NK cells in peripheral tissues and induces Treg cell differentiation(Nishimura H, 2001, Nishimura, et al., 2001). These data suggest that simultaneous blockade of the PD-1 and CTLA4 pathways on TILs may ultimately be required to drive optimal anti-tumor responses. Meanwhile, the combination of CTLA-4 inhibitor ipilimumab and PD-1 inhibitors nivolumab and

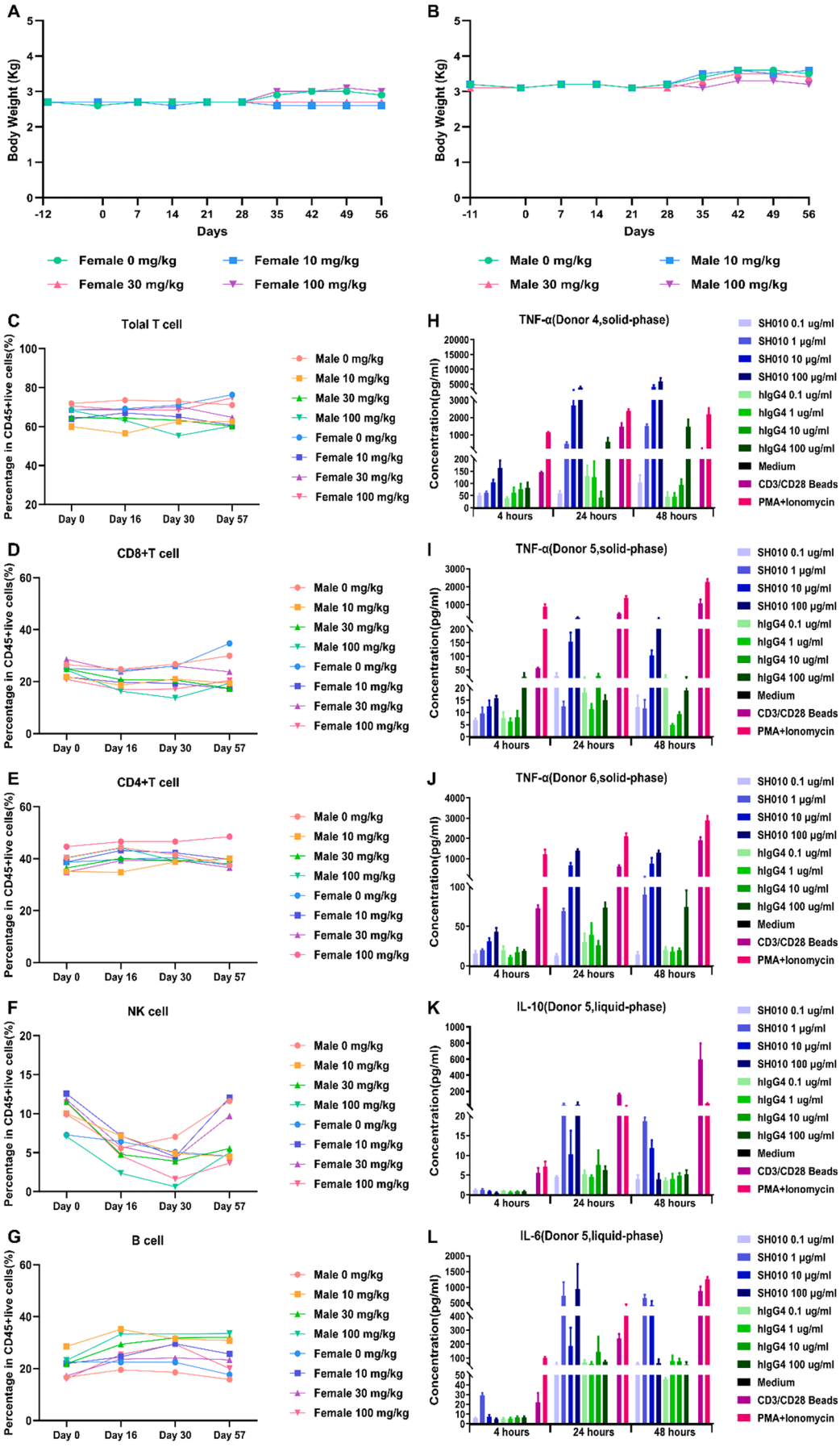

(caption on next page)

Fig.6. Safety Assessment of SH010. Average body weight (n = 5) of female (A) and male (B) cynomolgus monkeys subjected to repeated intravenous administration for 29 days with a subsequent recovery period of 28 days. Percentages of total T cells (C), CD8 + T cells (D), CD4 + T cells (E), NK cells (F), and B cells (G) among lymphocytes during repeated intravenous administration in cynomolgus monkeys. Results are presented as mean. The influence of SH010 on the secretion of TNF-α by hPBMC was assessed in donors 4 (H), 5 (I), and 6 (J) using the solid-phase detection system. The influence of SH010 on the secretion of IL-10 (K) and IL-6 (L) by hPBMC was assessed in donor 5 using the liquid-phase detection system.

pembrolizumab has been extensively studied in metastatic melanoma patients, and multiple clinical trials have demonstrated the effectiveness of the combined therapy(Hodi, et al., 2018, Long, et al., 2017, Tawbi, et al., 2018, Wolchok, et al., 2017). However, the dual-drug combination regimen, due to its excessive "power," can also lead to more serious adverse reactions(Hodi, et al., 2016, Kirchberger, et al., 2016, Meerveld-Eggink, et al., 2017, Weber, et al., 2016). Here, we demonstrate in *vitro* systems and tumor models that the bispecific antibody SH010, which blocks PD-L1 and CTLA-4, exhibits strong anti-tumor activity. Simultaneously, investigations were conducted regarding common safety issues in immune responses, such as Cytokine Release Syndrome (CRS).

In this study, we evaluated the capabilities of SH010 to block PD-1 and CTLA-4 in *vitro*, its potential to activate immune cells, and its anti-tumor effects in *vivo*. Demonstrating the cross-binding of SH010 with cynomolgus monkey PD-1/CTLA-4 provides a rationale for selecting cynomolgus monkeys as the species for safety assessment experiments. Additionally, it could bind to human PD-1/CTLA-4 and block the interaction of human PD-1 with PD-L1 and CTLA-4 with B7-1/CD86. This lays the foundation for SH010 to exert its immune checkpoint-blocking activity, activate immune cells, or exert anti-tumor functions, both in *vitro* and in *vivo*. Studies have shown that IL-2 and IFN-γ play essential roles in anti-tumor immune responses(Boyman and Sprent, 2012, Tau GZ, 2001). In the in *vitro* system, using SEB-activated human peripheral blood mononuclear cells (hPBMCs), SH010 significantly enhanced the secretion of IL-2/IFN-γ compared to Nivolumab, exhibiting a more pronounced immunostimulatory effect. In *vivo*, we utilized two xenograft models to assess the impact of SH010 on tumor growth in huPBMC-NCG mice. SH010 showed a significant inhibitory effect on tumor growth at the endpoint. This effect was statistically different from the solvent control, showing a dose-dependent relationship. However, it is regrettable that we did not perform efficacy comparisons of SH010 relative to the combination of anti-PD-1 and anti-CTLA-4. The main reason is that preclinical results may not accurately predict the performance in clinical trials. Therefore, we anticipate conducting such comparisons in clinical experiments. Overall, the results suggest that SH010 has the potential to block immune checkpoints, activate immune cells, and exert anti-tumor effects both in *vitro* and in *vivo*.

Antibody drugs are highly specific and biologically active, but due to their large size and poor membrane permeability, they are often unstable under gastrointestinal conditions. Therefore, they are administered through routes other than the gastrointestinal tract. The pharmacokinetics of antibody drugs, particularly following subcutaneous or intramuscular injections, involve unique characteristics such as limited distribution volume, convection transport, and nonlinear elimination. Each antibody drug shows different properties. It is crucial to conduct pharmacokinetic studies of antibody drugs to select appropriate dosages and administration regimens during clinical development. In this study, we administered SH010 to cynomolgus monkeys intravenously, both as a single intravenous infusion and repeatedly. The systemic exposure ($AUC_{0\text{-last}}$ and C_{max}) of SH010 in both male and female monkeys increased proportionally with the dose. At high doses, SH010 exhibited effective clearance without any apparent drug accumulation in the systemic exposure of both male and female monkeys. Simultaneously, addressing the observed decrease in systemic exposure, we speculated that the decline in exposure levels might be influenced by the presence of Anti-Drug Antibodies (ADAs).

Ensuring drug safety is crucial during the drug development process. In this study, we examined the average body weight and various immune parameters of male and female cynomolgus monkeys who received repeated intravenous infusions of SH010 at high, medium, and low doses for 29 days, followed by a 28-day recovery period. The experiment showed that there was a decrease in CD8 + T cells and NK cells during the administration period, but these levels returned to normal after drug administration stopped. Body weight, total T cells, CD4 + T cells, and B cells remained unchanged. CRS can occur when a large number of immune cells, especially T cells, are activated, and it can result in organ failure or death in severe cases.

MSD detection of SH010-stimulated human peripheral blood mononuclear cells (hPBMCs) from three different donors showed cytokine secretion of IFN-γ, TNF-α, IL-2, IL-4, IL-6, IL-8, and IL-10. In the solid-phase detection system, SH010 consistently induces TNF-α release in hPBMCs. However, in the liquid-phase detection system, TNF-α release from hPBMCs shows no significant difference compared to the negative controls (IgG4) and blank controls. The observed discrepancy in results may be attributed to methodological factors, indicating a potential limitation in accurately reflecting the impact of SH010 on TNF-α release in the detection method employed. In the liquid-phase detection system, SH010 induces the release of IL-6 from Donor 5 at 24 h and 48 h, as well as the release of IL-10 at 48 h. Conversely, this phenomenon was not observed in the solid-phase detection system, and there was no concentration-dependent trend, which might be caused by measurement errors. In addition, SH010 demonstrated no significant stimulatory effect on cytokine release from hPBMCs at various concentrations and treatment durations, resembling the negative control (IgG4) and blank control. These results highlight the superior safety profile of SH010.

5. Conclusions

In conclusion, our study examined a novel PD-1 and CTLA-4 bispecific antibody, SH010, which targets immune cells, boosts immune responses, and has anti-tumor effects. The pharmacokinetic and safety studies provide a foundation for further clinical research on SH010, offering an opportunity to improve cancer immunotherapy. At the same time, we also try other strategies to modify SH010 to produce better candidates.

CRediT authorship contribution statement

Qi Song: Writing – original draft, Investigation, Formal analysis, Conceptualization. **Meiling Jiang:** Investigation, Formal analysis, Conceptualization. **Xinrong Pan:** Investigation, Formal analysis. **Guanyue Zhou:** Investigation, Formal analysis. **Xiaomeng Zhang:** Writing – original draft, Conceptualization.

Declaration of competing interest

The authors declare that they have no known competing financial interests or personal relationships that could have appeared to influence the work reported in this paper.

Data availability

The data presented in this study are contained within the article.

Acknowledgement

This research did not receive any specific grant from funding agencies in the public, commercial, or not-for-profit sectors.

Animal Ethics Statement

All of our animal experiments are accredited by AAALAC International, and testing protocols, alterations, or operations involving the management and utilization of animals have been reviewed and sanctioned by the Institutional Animal Care and Use Committee (IACUC) before commencing. Veterinary technicians oversee animal welfare matters during testing. Approval number:IACUC-SW-B2021121-E010-01.

Appendix A. Supplementary data

Supplementary data to this article can be found online at https://doi.org/10.1016/j.imbio.2024.152844.

References

Boyman, O., Sprent, J., 2012. The role of interleukin-2 during homeostasis and activation of the immune system. Nature Reviews Immunology 12, 180.

Dovedi, S.J., Elder, M.J., Yang, C., Sitnikova, S.I., Irving, L., Hansen, A., Hair, J., Jones, D.C., Hasani, S., Wang, B., Im, S.-A., Tran, B., Subramaniam, D.S., Gainer, S. D., Vashisht, K., Lewis, A., Jin, X., Kentner, S., Mulgrew, K., Wang, Y., Overstreet, M. G., Dodgson, J., Wu, Y., Palazon, A., Morrow, M., Rainey, G.J., Browne, G.J., Neal, F., Murray, T.V., Toloczko, A.D., Dall'Acqua, W., Achour, I., Freeman, D.J., Wilkinson, R.W., Mazor, Y., 2021. Design and Efficacy of a Monovalent Bispecific PD-1/CTLA4 Antibody That Enhances CTLA4 Blockade on PD-1+ Activated T Cells. Cancer Discovery 11, 1100.

Gros, A., Robbins, P.F., Yao, X., Li, Y.F., Turcotte, S., Tran, E., Wunderlich, J.R., Mixon, A., Farid, S., Dudley, M.E., Hanada, K.-I., Almeida, J.R., Darko, S., Douek, D. C., Yang, J.C., Rosenberg, S.A., 2014. PD-1 identifies the patient-specific CD8+ tumor-reactive repertoire infiltrating human tumors. Journal of Clinical Investigation 124, 2246.

Hodi, F.S., Chesney, J., Pavlick, A.C., Robert, C., Grossmann, K.F., McDermott, D.F., Linette, G.P., Meyer, N., Giguere, J.K., Agarwala, S.S., Shaheen, M., Ernstoff, M.S., Minor, D.R., Salama, A.K., Taylor, M.H., Ott, P.A., Horak, C., Gagnier, P., Jiang, J., Wolchok, J.D., Postow, M.A., 2016. Combined nivolumab and ipilimumab versus ipilimumab alone in patients with advanced melanoma: 2-year overall survival outcomes in a multicentre, randomised, controlled, phase 2 trial. The Lancet Oncology 17, 1558.

Hodi, F.S., Chiarion-Sileni, V., Gonzalez, R., Grob, J.-J., Rutkowski, P., Cowey, C.L., Lao, C.D., Schadendorf, D., Wagstaff, J., Dummer, R., Ferrucci, P.F., Smylie, M., Hill, A., Hogg, D., Marquez-Rodas, I., Jiang, J., Rizzo, J., Larkin, J., Wolchok, J.D., 2018. Nivolumab plus ipilimumab or nivolumab alone versus ipilimumab alone in advanced melanoma (CheckMate 067): 4-year outcomes of a multicentre, randomised, phase 3 trial. The Lancet Oncology 19, 1480.

Hosseini, S.S., Khalili, S., Baradaran, B., Bidar, N., Shahbazi, M.-A., Mosafer, J., Hashemzaei, M., Mokhtarzadeh, A., Hamblin, M.R., 2021. Bispecific monoclonal antibodies for targeted immunotherapy of solid tumors: Recent advances and clinical trials. International Journal of Biological Macromolecules 167, 1030.

Kamphorst, A.O., Wieland, A., Nasti, T., Yang, S., Zhang, R., Barber, D.L., Konieczny, B. T., Daugherty, C.Z., Koenig, L., Yu, K., Sica, G.L., Sharpe, A.H., Freeman, G.J., Blazar, B.R., Turka, L.A., Owonikoko, T.K., Pillai, R.N., Ramalingam, S.S., Araki, K., Ahmed, R., 2017. Rescue of exhausted CD8 T cells by PD-1–targeted therapies is CD28-dependent. Science 355, 1423.

Keam, S.J., 2022. Cadonilimab: First Approval. Drugs 82, 1333.

Kennedy, P.T., Saulters, E.L., Duckworth, A.D., Lim, Y.J., Woolley, J.F., Slupsky, J.R., Cragg, M.S., Ward, F.J., Dahal, L.N., 2024. Soluble CTLA-4 attenuates T cell activation and modulates anti-tumor immunity. Molecular Therapy 32, 457.

Kirchberger, M.C., Hauschild, A., Schuler, G., Heinzerling, L., 2016. Combined low-dose ipilimumab and pembrolizumab after sequential ipilimumab and pembrolizumab failure in advanced melanoma. European Journal of Cancer 65, 182.

Larkin, J., Chiarion-Sileni, V., Gonzalez, R., Grob, J.J., Cowey, C.L., Lao, C.D., Schadendorf, D., Dummer, R., Smylie, M., Rutkowski, P., Ferrucci, P.F., Hill, A., Wagstaff, J., Carlino, M.S., Haanen, J.B., Maio, M., Marquez-Rodas, I., McArthur, G. A., Ascierto, P.A., Long, G.V., Callahan, M.K., Postow, M.A., Grossmann, K., Sznol, M., Dreno, B., Bastholt, L., Yang, A., Rollin, L.M., Horak, C., Hodi, F.S., Wolchok, J.D., 2015. Combined Nivolumab and Ipilimumab or Monotherapy in Untreated Melanoma. New England Journal of Medicine 373, 23.

Ljunggren, H.G., Jonsson, R., Höglund, P., 2018. Seminal immunologic discoveries with direct clinical implications: The 2018 Nobel Prize in Physiology or Medicine honours discoveries in cancer immunotherapy. Scandinavian Journal of Immunology 88.

Long, G.V., Atkinson, V., Cebon, J.S., Jameson, M.B., Fitzharris, B.M., McNeil, C.M., Hill, A.G., Ribas, A., Atkins, M.B., Thompson, J.A., Hwu, W.-J., Hodi, F.S., Menzies, A.M., Guminski, A.D., Kefford, R., Kong, B.Y., Tamjid, B., Srivastava, A., Lomax, A.J., Islam, M., Shu, X., Ebbinghaus, S., Ibrahim, N., Carlino, M.S., 2017. Standard-dose pembrolizumab in combination with reduced-dose ipilimumab for patients with advanced melanoma (KEYNOTE-029): an open-label, phase 1b trial. The Lancet Oncology 18, 1202.

Mandel, I., Haves Ziv, D., Goldshtein, I., Peretz, T., Alishekevitz, D., Fridman Dror, A., Hakim, M., Hashmueli, S., Friedman, I., Sapir, Y., Greco, R., Qu, H., Nestle, F., Wiederschain, D., Pao, L., Sharma, S., Ben Moshe, T., 2022. BND-22, a first-in-class humanized ILT2-blocking antibody, promotes antitumor immunity and tumor regression. J Immunother Cancer 10.

Meerveld-Eggink, A., Rozeman, E.A., Lalezari, F., van Thienen, J.V., Haanen, J.B.A.G., Blank, C.U., 2017. Short-term CTLA-4 blockade directly followed by PD-1 blockade in advanced melanoma patients: a single-center experience. Annals of Oncology 28, 862.

Nishimura, H., Okazaki, T., Tanaka, Y., Nakatani, K., Hara, M., Matsumori, A., Sasayama, S., Mizoguchi, A., Hiai, H., Minato, N., Honjo, T., 2001. Autoimmune Dilated Cardiomyopathy in PD-1 Receptor-Deficient Mice. Science 291, 319.

Pang, X., Huang, Z., Zhong, T., Zhang, P., Wang, Z.M., Xia, M., Li, B. 2023. Cadonilimab, a tetravalent PD-1/CTLA-4 bispecific antibody with trans-binding and enhanced target binding avidity. mAbs 15.

Pardoll, D.M., 2012. The blockade of immune checkpoints in cancer immunotherapy. Nature Reviews Cancer 12, 252.

Perez-Santos, M., 2020. Bispecific anti-PD-1/CTLA-4 antibody for advanced solid tumors. Pharmaceutical Patent Analyst 9, 149.

Postow, M.A., Chesney, J., Pavlick, A.C., Robert, C., Grossmann, K., McDermott, D., Linette, G.P., Meyer, N., Giguere, J.K., Agarwala, S.S., Shaheen, M., Ernstoff, M.S., Minor, D., Salama, A.K., Taylor, M., Ott, P.A., Rollin, L.M., Horak, C., Gagnier, P., Wolchok, J.D., Hodi, F.S., 2015. Nivolumab and Ipilimumab versus Ipilimumab in Untreated Melanoma. New England Journal of Medicine 372, 2006.

Qureshi, O.S., Zheng, Y., Nakamura, K., Attridge, K., Manzotti, C., Schmidt, E.M., Baker, J., Jeffery, L.E., Kaur, S., Briggs, Z., Hou, T.Z., Futter, C.E., Anderson, G., Walker, L.S.K., Sansom, D.M., 2011. Trans-Endocytosis of CD80 and CD86: A Molecular Basis for the Cell-Extrinsic Function of CTLA-4. Science 332, 600.

Qureshi, O.S., Kaur, S., Hou, T.Z., Jeffery, L.E., Poulter, N.S., Briggs, Z., Kenefeck, R., Willox, A.K., Royle, S.J., Rappoport, J.Z., Sansom, D.M., 2012. Constitutive Clathrin-mediated Endocytosis of CTLA-4 Persists during T Cell Activation. Journal of Biological Chemistry 287, 9429.

Raskov, H., Orhan, A., Christensen, J.P., Gögenur, I., 2020. Cytotoxic CD8+ T cells in cancer and cancer immunotherapy. British Journal of Cancer 124, 359.

Tawbi, H.A., Forsyth, P.A., Algazi, A., Hamid, O., Hodi, F.S., Moschos, S.J., Khushalani, N.I., Lewis, K., Lao, C.D., Postow, M.A., Atkins, M.B., Ernstoff, M.S., Reardon, D.A., Puzanov, I., Kudchadkar, R.R., Thomas, R.P., Tarhini, A., Pavlick, A. C., Jiang, J., Avila, A., Demelo, S., Margolin, K., 2018. Combined Nivolumab and Ipilimumab in Melanoma Metastatic to the Brain. New England Journal of Medicine 379, 722.

Weber, J.S., Gibney, G., Sullivan, R.J., Sosman, J.A., Slingluff, C.L., Lawrence, D.P., Logan, T.F., Schuchter, L.M., Nair, S., Fecher, L., Buchbinder, E.I., Berghorn, E., Ruisi, M., Kong, G., Jiang, J., Horak, C., Hodi, F.S., 2016. Sequential administration of nivolumab and ipilimumab with a planned switch in patients with advanced melanoma (CheckMate 064): an open-label, randomised, phase 2 trial. The Lancet Oncology 17, 943.

Wolchok, J.D., Kluger, H., Callahan, M.K., Postow, M.A., Rizvi, N.A., Lesokhin, A.M., Segal, N.H., Ariyan, C.E., Gordon, R.-A., Reed, K., Burke, M.M., Caldwell, A., Kronenberg, S.A., Agunwamba, B.U., Zhang, X., Lowy, I., Inzunza, H.D., Feely, W., Horak, C.E., Hong, Q., Korman, A.J., Wigginton, J.M., Gupta, A., Sznol, M., 2013. Nivolumab plus Ipilimumab in Advanced Melanoma. New England Journal of Medicine 369, 122.

Wolchok, J.D., Chiarion-Sileni, V., Gonzalez, R., Rutkowski, P., Grob, J.-J., Cowey, C.L., Lao, C.D., Wagstaff, J., Schadendorf, D., Ferrucci, P.F., Smylie, M., Dummer, R., Hill, A., Hogg, D., Haanen, J., Carlino, M.S., Bechter, O., Maio, M., Marquez-Rodas, I., Guidoboni, M., McArthur, G., Lebbé, C., Ascierto, P.A., Long, G.V., Cebon, J., Sosman, J., Postow, M.A., Callahan, M.K., Walker, D., Rollin, L., Bhore, R., Hodi, F.S., Larkin, J., 2017. Overall Survival with Combined Nivolumab and Ipilimumab in Advanced Melanoma. New England Journal of Medicine 377, 1345.